Introducing proton/electron mediators enhances catalytic ability of iron porphyrin complex for photochemical CO2 reduction

COMMUNICATION

Introducing proton/electron mediators enhances catalytic ability of iron porphyrin complex for photochemical CO_2 reduction

Maho Imai,[a‡] Kento Kosugi,[a‡] Yutaka Saga,[a] Mio Kondo [*abc] and Shigeyuki Masaoka [*ab]

A novel iron porphyrin complex with hydroquinone moieties as proton/electron mediators at *meso* positions was designed and synthesised. The complex serves as an efficient catalyst for photochemical CO_2 reduction, and its turnover frequency (TOF = 1.3 × 10^4 h^{−1}) was the highest among those of comparable systems with sufficient durability.

The catalytic reduction of CO_2 is attractive as a solution for energy and environmental issues since this reaction (i.e. CO_2 + $2H^+$ + $2e^-$ → CO + H_2O) converts the greenhouse gas CO_2 into valuable chemical resources.[1] Thus far, many molecule-based catalysts for CO_2 reduction have been developed.[2–17] Among them, iron porphyrin complexes are fascinating candidates because of their high activity, selectivity, and robustness (Fig. 1a).[3–16] Another important feature of porphyrin scaffolds is that a variety of functional groups can be installed at *meso* positions. To date, various efforts have been devoted to enhancing the activity of iron porphyrin complexes by modifying the *meso* position functional groups.[4–16] Of particular interest is the introduction of proton mediators (local proton sources) close to the catalytic centre[5–12] because CO_2 reduction occurs via multi-proton transfer processes. A representative example of such a catalyst is an iron porphyrin complex bearing hydroxyphenyl groups at *meso* positions, 5,10,15,20-tetrakis(2,6-dihydroxyphenyl)porphyrinato iron(III) chloride (**CAT**, Fig. 1b).[5] This complex exhibits the highest catalytic activity for photochemical CO_2 reduction among previously reported iron porphyrin complexes.[12] This finding clearly demonstrates that

(a) Iron porphyrin complex
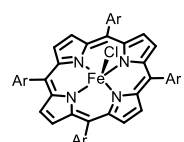
✔ High activity & selectivity
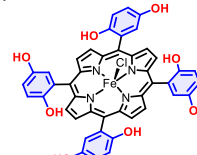✔ Robustness
✔ Modification at *meso* positions is possible

(b) Previous work
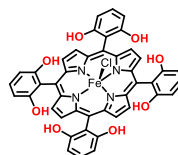
CAT

Proton mediators

(c) This work

Fe1

Proton/Electron mediators

Fig. 1 Characteristics of (a) iron porphyrin complexes, and the iron porphyrin complexes prepared in (b) previous work, and (c) this study.

the introduction of functional groups that facilitate elemental reactions of CO_2 reduction is a strategy that has excellent potential for catalytic activity enhancement. Given that CO_2 reduction involves electron transfer as well as proton transfer, the introduction of proton/electron mediators should lead to further improvements in catalytic activity. However, there are no reports of porphyrin-based catalysts with proton/electron mediator functional groups for photochemical CO_2 reduction.

Herein, we report a novel iron porphyrin complex bearing proton/electron mediators at the *meso* positions. Using this complex as a catalyst, a catalytic system for photochemical CO_2 reduction was constructed. The activity of our system was demonstrated to be superior to that of a system based on the iron porphyrin complex bearing only proton mediators, **CAT**, which exhibits the highest catalytic activity for photochemical CO_2 reduction among previously reported iron porphyrin complexes. Moreover, the turnover frequency (TOF) of our CO production system is the highest among relevant similar systems.

The key to our success was the introduction of hydroquinone moieties at the *meso* positions of the iron

a. *Division of Applied Chemistry, Graduate School of Engineering Osaka University 2-1 Yamadaoka, Suita Osaka 565-0871, Japan. E-mail: mio@chem.eng.osaka-u.ac.jp, masaoka@chem.eng.osaka-u.ac.jp.*
b. *Innovative Catalysis Science Division, Institute for Open and Transdisciplinary Research Initiatives (ICS-OTRI), Osaka University, Suita, Osaka 565-0871, Japan.*
c. *PRESTO, Japan Science and Technology Agency (JST), 4-1-4 Honcho, Kawaguchi, Saitama 332-0012, Japan.*
†Electronic Supplementary Information (ESI) available: Experimental details, UV–vis absorption spectroscopy, Electrochemical measurements, Photocatalytic activity for CO_2 reduction, Quantum chemical calculation, Emission quenching experiments, Comparison of catalytic ability. See DOI: 10.1039/x0xx00000x
‡ These authors contributed equally.

porphyrin complex. Hydroquinone is known to act as both a proton-responsive and electron-responsive site.[18] Therefore, the hydroquinone moieties introduced in the vicinity of the active centre are expected to act as proton/electron mediators in CO_2 reduction reactions.

Based on the aforementioned considerations, we designed a new iron complex, 5,10,15,20-tetrakis(2,5-dihydroxyphenyl)porphyrinato iron(III) chloride (**Fe1**) (Fig. 1c). It should be noted that **Fe1** is a structural isomer of the benchmark iron porphyrin catalyst, **CAT**. **Fe1** was synthesised according to the procedure shown in Scheme S1 (Electronic Supplementary Information). First, a free base porphyrin, 5,10,15,20-tetrakis(2,5-dihydroxyphenyl)porphyrin (**1**), was synthesised,[5,19] and Fe was inserted into **1** via a slightly modified previously reported method.[5] The synthesised **Fe1** was characterised by elemental analysis, UV–vis absorption spectroscopy, and MALDI spiral-TOFMS. In the UV–vis absorption spectrum of **Fe1**, bands attributed to the hydroquinone moieties at 220 and 299 nm, as well as a Soret band associated with the porphyrin scaffold at 415 nm, were observed (Fig. S23a,b). In addition, Q-bands, which are also characteristic of porphyrin derivatives,[20] appeared at maximum wavelengths, λ_{max}, of 506, 584, and 664 nm in the spectrum of **Fe1**. Notably, there were fewer Q-bands in the spectrum of **Fe1** than in the spectrum of **1** (λ_{max} = 511, 545, 585, and 646 nm; Fig. S23c), suggesting that the former had greater porphyrin ring symmetry.[20] This result, together with the elemental analysis results, confirmed that an iron ion had been inserted into the porphyrin ring of **1**.

To investigate the electrochemical properties of **Fe1**, cyclic voltammetry (CV) measurements were performed in a 0.10 M tetra-*n*-butylammonium perchlorate (TBAP)/*N*,*N*-dimethylformamide (DMF) solution. Under an Ar atmosphere, **Fe1** exhibited three redox waves, at −0.72, −1.60, and −2.11 V [vs. ferrocene/ferrocenium (Fc/Fc$^+$)] (Fig. 2a). For comparison, the cyclic voltammogram of the iron porphyrin complex without hydroquinone moieties, 5,10,15,20-tetrakis(phenyl)porphyrinato iron(III) chloride (**FeTPP-Cl**), was measured (Fig. S24). By comparing the voltammogram with that of **FeTPP-Cl**, three redox waves in the voltammogram of **Fe1**, observed at −0.72, −1.60, and −2.11 V, were assigned to Fe^{III}/Fe^{II}, Fe^{II}/Fe^I, and Fe^I/Fe^0 redox couples, respectively (Table S1).[3d] Previous work suggested that the irreversible reduction wave at −1.1 V was due to the interaction between the iron porphyrin complex and hydroquinone moieties.[21]

Subsequently, we obtained cyclic voltammograms of **Fe1** in a CO_2 atmosphere. An increase in the irreversible current was observed approximately at −2.03 V, indicating that **Fe1** and CO_2 interacted at this potential (Fig. 2b, yellow line). Moreover, the intensity of the irreversible current increased in the presence of 0.10 M trifluoroethanol (TFE) as a proton source (Fig. 2b, red line). These results suggest that **Fe1** exhibits catalytic activity for CO_2 reduction.

Encouraged by these electrochemical measurement results, we investigated the catalytic activity of **Fe1** for photochemical CO_2 reduction using our custom-made photoreactor (Fig. S25). The photochemical reaction was
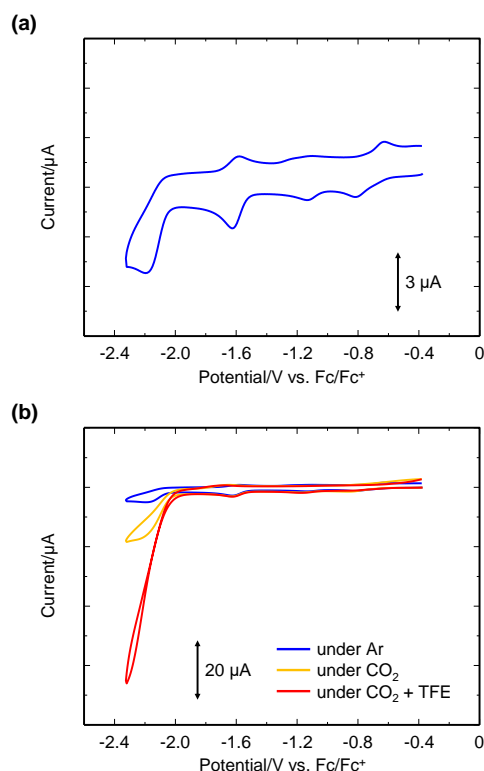

(a)

(b)

Fig. 2 (a) Cyclic voltammogram of **Fe1** (0.20 mM) in DMF with TBAP (0.10 M) under Ar. (b) Cyclic voltammograms of **Fe1** (0.20 mM) in DMF with TBAP (0.10 M) under Ar (blue line), CO_2 (yellow line), and CO_2 in the presence of TFE (0.10 M) (red line). [Working electrode: glassy carbon; counter electrode: Pt wire; scan rate: 100 mV s^{-1}.]

conducted under visible-light irradiation (400 ≤ λ ≤ 750 nm) in a CO_2-saturated acetonitrile (MeCN) solution containing **Fe1** (2.0 μM) as the catalyst, Ir(ppy)$_3$ (Hppy = 2-phenylpyridine, 20 μM) as a photosensitiser, 1,3-dimethyl-2-phenyl-2,3-dihydro-1*H*-benzo[*d*]-imidazole (BIH, 0.10 M) as a sacrificial electron donor, and TFE (0.10 M) as a proton source. After 1 h of photoirradiation, the product was quantified using gas chromatography, and the formation of CO (51.8 μmol) was confirmed. The turnover number (TON) for CO production was 1.3 × 10^4 (Table 1, Entry 1 and Fig. S26). In this photocatalytic reaction, it was confirmed that H_2 was not formed, indicating the excellent selectivity of **Fe1**.

To verify the role of each component in the photoreaction, a series of control experiments was conducted. CO was not detected when the reaction was performed without **Fe1**, without Ir(ppy)$_3$, without BIH, under Ar, or in the dark (Table 1, Entries 2–6). These results confirm that **Fe1** is the catalyst, Ir(ppy)$_3$ functions as a photosensitiser, BIH acts as a sacrificial electron donor, and CO_2 is the substrate. An isotopic labelling experiment under a $^{13}CO_2$ atmosphere was also conducted, and ^{13}CO was generated, demonstrating that the detected CO was a product of CO_2 reduction (Fig. 3).

Subsequently, we investigated the effects of the proton/electron mediators introduced close to the active centre. In this study, we compared the catalytic activity of **Fe1** with that of a benchmark catalyst, **CAT**, which is a structural isomer of **Fe1** but contains only proton mediators. The TON of

ChemComm

COMMUNICATION

Table 1 Control experiments for photochemical CO_2 reduction by **Fe1** for 1 h

Entry	Catalyst[a]	Photosensitiser[b]	Electron donor[c]	Gas	Light[d]/nm	Medium	TON	
							CO	H_2
1	**Fe1**	Ir(ppy)$_3$	BIH	CO_2	$400 \leq \lambda \leq 750$	0.10 M TFE/MeCN	1.3×10^4	0
2	-	Ir(ppy)$_3$	BIH	CO_2	$400 \leq \lambda \leq 750$	0.10 M TFE/MeCN	0	0
3	**Fe1**	-	BIH	CO_2	$400 \leq \lambda \leq 750$	0.10 M TFE/MeCN	0	0
4	**Fe1**	Ir(ppy)$_3$	-	CO_2	$400 \leq \lambda \leq 750$	0.10 M TFE/MeCN	0	0
5	**Fe1**	Ir(ppy)$_3$	BIH	Ar	$400 \leq \lambda \leq 750$	0.10 M TFE/MeCN	0	4
6	**Fe1**	Ir(ppy)$_3$	BIH	CO_2	dark	0.10 M TFE/MeCN	0	0

[a]2.0 μM **Fe1**. [b]20 μM Ir(ppy)$_3$. [c]0.10 M BIH [d]Xe lamp (150 W) with long pass filter.

CAT for CO production was found to be 1.0×10^3 for 1 h (TOF = 1.0×10^3 h^{-1}) under identical experimental conditions, and a significant difference in the catalytic activities of the **Fe1** and **CAT** iron porphyrin complexes was observed (Fig. 4 and Table S2). This result indicates that the catalytic activity was enhanced by introducing proton/electron mediators in the vicinity of catalytic centre without changing constituent elements.

For further investigation of the effect of hydroquinone moieties, several attempts were made. Our experimental results clearly demonstrate that our new catalyst with hydroquinone moieties, **Fe1**, exhibits superior catalytic activity compared to its positional isomer, **CAT**. We have hypothesized there are mainly three possibilities to explain the improved performance of our catalyst; (a) shift in redox potentials of the catalytic centre (i.e., change in the reactivity of catalytic centre) by the introduction of hydroquinone moieties, (b) the effect of proton relay ability, and (c) the effect of electron relay ability by the hydroquinone moieties. First, the redox potential of **Fe1** to produce catalytically active species was the same as that of **CAT** (Table S1),[10] indicating that the introduction of hydroquinone moieties does not affect the reactivity of the catalytic centre. Second, quantum chemical calculation was performed to optimize the structure of the CO_2 adduct of the Fe^0 state of **Fe1**. The result revealed that the hydroquinone moieties can interact with CO_2 through hydrogen bonding (Fig. S27). Similar interaction that stabilizes CO_2 adduct has also been reported for **CAT**.[6] This suggested that there should be no significant

difference in proton relay ability between **Fe1** and **CAT**. Third, we conducted emission quenching experiments to investigate the effect of hydroquinone moieties on electron transfer processes. As a result, emission quenching of the photosensitiser, Ir(ppy)$_3$, was observed in the presence of hydroquinone and one equivalent of 1,8-diazabicyclo[5.4.0]-7-undecene (DBU) as a base (Fig. S28). On the other hand, emission quenching was hardly observed in the presence of hydroquinone or DBU (Fig. S29). These results imply that the hydroquinone moieties of **Fe1** were involved in the electron transfer process after deprotonation, indicating the effect of the electron relay ability of the hydroquinone moieties on the catalysis.

Finally, we compared the catalytic ability of **Fe1** with those of relevant similar systems. In terms of catalytic activity, the TOF for photochemical CO_2 reduction of **Fe1** (1.3×10^4 h^{-1}) is higher than those of all other iron porphyrin complexes reported in the literature (Table S3 and Fig. S30).[3c,11–16] Moreover, the TON of **Fe1** is the highest class among previously reported iron-complex-based catalysts, indicating the durability of **Fe1** during photocatalysis (Table S4).[3c,11–17] These results clearly demonstrate that the introduction of proton/electron mediators in the vicinity of the active centre is an effective strategy for developing highly efficient catalysts for CO_2 reduction.

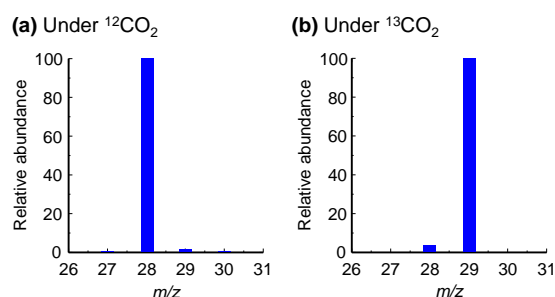In summary, we report a novel iron porphyrin complex bearing hydroquinone moieties at *meso* positions as

Fig. 3 Mass spectra of CO generated using MeCN solution containing 2.0 μM **Fe1**, 20 μM Ir(ppy)$_3$, 0.10 M BIH, and 0.10 M TFE at 20 °C during irradiation with a Xe lamp ($400 \leq \lambda \leq 750$ nm) over a period of 75 min in (a) $^{12}CO_2$ and (b) $^{13}CO_2$ atmospheres.
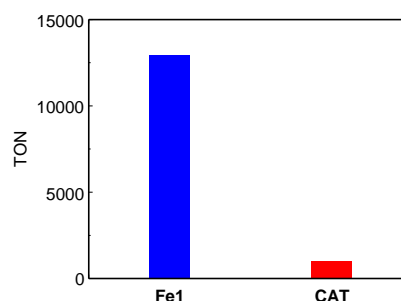

Fig. 4 Photochemical CO_2 reduction activities for CO production using a CO_2-saturated MeCN solution containing 2.0 μM **Fe1** (blue) or 2.0 μM **CAT** (red), 20 μM Ir(ppy)$_3$, 0.10 M BIH, and 0.10 M TFE at 20 °C with Xe lamp ($400 \leq \lambda \leq 750$ nm) irradiation.

proton/electron mediators (**Fe1**). **Fe1** exhibits high activity for CO_2 reduction under visible light irradiation. The TOF of **Fe1** for CO production was 1.3×10^4 h^{-1}, which is significantly higher than that of the iron porphyrin complex bearing only proton mediators, **CAT**, which is a structural isomer of **Fe1**. It is worth noting that **Fe1** exhibited a TOF that was higher than that of any other iron porphyrin complex reported in the literature. Moreover, the TON of **Fe1** was the highest class among iron-complex-based catalysts of photochemical CO_2 reduction. Thus, collectively, these results indicate the effectiveness of our novel strategy for the development of highly efficient CO_2 reduction catalysts.

Conflicts of interest

There are no conflicts to declare.

Notes and references

1 A. M. Appel, J. E. Bercaw, A. B. Bocarsly, H. Dobbek, D. L. DuBois, M. Dupuis, J. G. Ferry, E. Fujita, R. Hille, P. J. A. Kenis, C. A. Kerfeld, R. H. Morris, C. H. F. Peden, A. R. Portis, S. W. Ragsdale, T. B. Rauchfuss, J. N. H. Reek, L. C. Seefeldt, R. K. Thauer and G. L. Waldrop, *Chem. Rev.*, 2013, **113**, 6621.
2 (a) H. Takeda, C. Cometto, O. Ishitani and M. Robert, *ACS Catal.*, 2017, **7**, 70. (b) R. Francke, B. Schille and M. Roemelt, *Chem. Rev.*, 2018, **118**, 4631. (c) E. Boutin, L. Merakeb, B. Ma, B. Boudy, M. Wang, J. Bonin, E. Anxolabéhère-Mallart and M. Robert, *Chem. Soc. Rev.*, 2020, **49**, 5772.
3 (a) M. Hammouche, D. Lexa, J. M. Savéant and M. Momenteau, *J. Electronal. Chem. Interfacial Electrochem.*, 1988, **249**, 347. (b) I. Bhugun, D. Lexa and J. M. Savéant, *J. Am. Chem. Soc.*, 1994, **116**, 5015. (c) T. Dhanasekaran, J. Grodkowski, P. Neta, P. Hambright and E. Fujita, *J. Phys. Chem. A*, 1999, **103**, 7742. (d) C. Costentin, S. Drouet, G. Passard, M. Robert and J. M. Savéant, *J. Am. Chem. Soc.*, 2013, **135**, 9023. (e) J. Bonin, M. Chaussemier, M. Robert and M. Routier, *ChemCatChem*, 2014, **6**, 3200. (f) K. Kosugi, M. Kondo and S. Masaoka, *Angew. Chem. Int. Ed.*, 2021, **60**, 22070.
4 (a) P. Gotico, Z. Halime and A. Aukauloo, *Dalton Trans.*, 2020, **49**, 2381. (b) P. Saha, S. Amanullah and A. Dey, *Acc. Chem. Res.*, 2022, **55**, 134. (c) I. Azcarate, C. Costentin, M. Robert and J. M. Savéant, *J. Am. Chem. Soc.*, 2016, **138**, 16639. (d) A. Khadhraoui, P. Gotico, B. Boitrel, W. Leibl, Z. Halime and A. Aukauloo, *Chem. Commun.*, 2018, **54**, 11630. (e) E. M. Nichols,

J. S. Derrick, S. K. Nistanaki, P. T. Smith and C. J. Chang, *Chem. Sci.*, 2018, **9**, 2952.
5 C. Costentin, S. Drouet, M. Robert and J. M. Savéant, *Science*, 2012, **338**, 90.
6 C. Costentin, G. Passard, M. Robert and J. M. Savéant, *J. Am. Chem. Soc.*, 2014, **136**, 11821.
7 C. Costentin, G. Passard, M. Robert and J. M. Savéant, *Proc. Natl. Acad. Sci. USA*, 2014, **111**, 14990.
8 S. Sinha and J. J. Warren, *Inorg. Chem.*, 2018, **57**, 12650.
9 C. G. Margarit, C. Schnedermann, N. G. Asimow and D. G. Nocera, *Organometallics*, 2019, **38**, 1219.
10 A. Sonea, K. L. Branch and J. J. Warren, *ACS Catal.*, 2023, **13**, 3902.
11 J. Bonin, M. Robert and M. Routier, *J. Am. Chem. Soc.*, 2014, **136**, 16768.
12 H. Yuan, B. Cheng, J. Lei, L. Jiang and Z. Han, *Nat. Commun.*, 2021, **12**, 1835.
13 J. Grodkowski and P. Neta, *J. Phys. Chem. A*, 2000, **104**, 4475.
14 H. Rao, L. C. Schmidt, J. Bonin and M. Robert, *Nature*, 2017, **548**, 74.
15 E. Pugliese, P. Gotico, I. Wehrung, B. Boitrel, A. Quaranta, M.-H. Ha-Thi, T. Pino, M. Sircoglou, W. Leibl, Z Halime and A. Aukauloo, *Angew. Chem. Int. Ed.*, 2022, **61**, e202117530.
16 A. Stoumpidi, A. Trapali, M. Poisson, A. Barrozo, S. Bertaina, M. Orio, G. Charalambidis and A. G. Coutsolelos, *ChemCatChem*, 2023, **15**, e202200856.
17 (a) J. Grodkowski, P. Neta, E. Fujita, A. Mahammed, L. Simkhovich, and Z. Gross, *J. Phys. Chem. A*, 2002, **106**, 4772. (b) H. Takeda, K. Ohashi, A. Sekine and O. Ishitani, *J. Am. Chem. Soc.*, 2016, **138**, 4354. (c) A. Rosas-Hernández, P. G. Alsabeh, E. Barsch, H. Junge, R. Ludwigab and M. Beller, *Chem. Commun.*, 2016, **52**, 8393. (d) Z. Guo, S. Cheng, C. Cometto, E. Anxolabéhère-Mallart, S.-M. Ng, C.-C. Ko, G. Liu, L. Chen, M. Robert and T.-C. Lau, *J. Am. Chem. Soc.*, 2016, **138**, 9413. (e) A. Rosas-Hernández, C. Steinlechner, H. Junge and M. Beller, *Green Chem.*, 2017, **19**, 2356. (f) Y. Sakaguchi, A. Call, M. Cibian, K. Yamauchi and K. Sakai, *Chem. Commun.*, 2019, **55**, 8552. (g) L. Chen, Y. Qin, G. Chen, M. Li, L. Cai, Y. Qiu, H. Fan, M. Robert and T.-C. Lau, *Dalton Trans.*, 2019, **48**, 9596. (h) P. A. Forero-Cortés, M. Marx, N. G. Moustakas, F. Brunner, C. E. Housecroft, E. C. Constable, H. Junge, M. Beller and J. Strunk, *Green Chem.*, 2020, **22**, 4541. (i) Y. Qin, L. Chen, G. Chen, Z. Guo, L. Wang, H. Fan, M. Robert and T.-C. Lau, *Chem. Commun.*, 2020, **56**, 6249. (j) Y. Wang, X.-W. Gao, J. Li and D. Chao, *Chem. Commun.*, 2020, **56**, 12170. (k) Y. Wang, L. Chen, T. Liu and D. Chao, *Dalton Trans.*, 2021, **50**, 6273. (l) H. Takeda, Y. Monma and O. Ishitani, *ACS Catal.*, 2021, **11**, 11973. (m) Y. Wang, T. Liu, L. Chen and D. Chao, *Inorg. Chem.*, 2021, **60**, 5590. (n) P. De La Torre, J. S. Derrick, A. Snider, P. T. Smith, M. Loipersberger, M. Head-Gordon and C. J. Chang, *ACS Catal.*, 2022, **12**, 8484. (o) J.-W. Wang, F. Ma, T. Jin, P. He, Z.-M. Luo, S. Kupfer, M. Karnahl, F. Zhao, Z. Xu, T. Jin, T. Lian, Y.-L. Huang, L. Jiang, L.-Z. Fu, G. Ouyang and X.-Y. Yi, *J. Am. Chem. Soc.*, 2023, **145**, 676. (p) L. An, P. De La Torre, P. T. Smith, M. R. Narouz and C. J. Chang, *Angew. Chem. Int. Ed.*, 2023, **62**, e202209396.
18 J. J. Warren, T. A. Tronic and J. M. Mayer, *Chem. Rev.*, 2010, **110**, 6961.
19 P. Bhyrappa, S. R. Wilson and K. S. Suslick, *J. Am. Chem. Soc.*, 1997, **119**, 8492.
20 M. Gouterman, *J. Mol. Spectrosc.*, 1961, **6**, 138.
21 K. Kosugi, M. Imai, M. Kondo and S. Masaoka, *Chem. Lett.*, 2022, **51**, 224.